

Nonlocal vibration analysis of FG nano beams with different boundary conditions

Javad Ehyaei*, Farzad Ebrahimi and Erfan Salari

*Department of Mechanical Engineering, Faculty of Engineering, Imam Khomeini International
University, Qazvin, Iran*

(Received December 24, 2015, Revised May 18, 2016, Accepted May 21, 2016)

Abstract. In this paper, the classical and non-classical boundary conditions effect on free vibration characteristics of functionally graded (FG) size-dependent nanobeams are investigated by presenting a semi analytical differential transform method (DTM) for the first time. Three kinds of mathematical models, namely; power law (P-FGM), sigmoid (S-FGM) and Mori-Tanaka (MT-FGM) distribution are considered to describe the material properties in the thickness direction. The nonlocal Eringen theory takes into account the effect of small size, which enables the present model to become effective in the analysis and design of nanosensors and nanoactuators. Governing equations are derived through Hamilton's principle and they are solved applying semi analytical differential transform method. The good agreement between the results of this article and those available in literature validated the presented approach. The detailed mathematical derivations are presented and numerical investigations are performed while the emphasis is placed on investigating the effect of the several parameters such as small scale effects, spring constant factors, various material compositions and mode number on the normalized natural frequencies of the FG nanobeams in detail. It is explicitly shown that the vibration of FG nanobeams is significantly influenced by these effects. Numerical results are presented to serve as benchmarks for future analyses of FG nanobeams.

Keywords: DT method; functionally graded material; non-classical boundary condition; nanobeams; vibration

1. Introduction

Functionally graded materials (FGMs) are composite materials with inhomogeneous micromechanical structure. They are generally composed of two different parts such as ceramic with excellent characteristics in heat and corrosive resistances and metal with toughness. The material properties of FGMs change smoothly between two surfaces and the advantages of this combination lead to novel structures which can withstand in large mechanical loadings under high temperature environments. Presenting novel properties, FGMs have attracted intensive research interests, which were mainly focused on their static, dynamic and vibration characteristics of FG structures.

Moreover, structural elements such as beams, plates, and membranes in micro or nanolength scale are commonly used as components in micro/nano electromechanical systems

*Corresponding author, Ph.D., E-mail: jehyaei@eng.ikiu.ac.ir

(MEMS/NEMS). Therefore understanding the mechanical and physical properties of nanostructures is necessary for its practical applications. Nanoscale engineering materials have attracted great interest in modern science and technology after the invention of carbon nanotubes (CNTs). They have significant mechanical, thermal and electrical performances that are superior to the conventional structural materials. In recent years, nanobeams and CNTs hold a wide variety of potential applications (Zhang *et al.* 2004, Wang 2005, Wang and Varadan (2006) such as sensors, actuators, transistors, probes, and resonators in NEMSs. For instance, in MEMS/NEMS; nanostructures have been used in many areas including communications, machinery, information technology and biotechnology technologies.

Since conducting experiments at the nanoscale is a daunting task, and atomistic modeling is restricted to small-scale systems owing to computer resource limitations, continuum mechanics offers an easy and useful tool for the analysis of CNTs. However the classical continuum models need to be extended to consider the nanoscale effects and this can be achieved through the nonlocal elasticity theory proposed by Eringen (1972) which consider the size-dependent effect. According to this theory, the stress state at a reference point is considered as a function of strain states of all points in the body. This nonlocal theory is proved to be in accordance with atomic model of lattice dynamics and with experimental observations on phonon dispersion Eringen (1983).

Moreover, in recent years the application of nonlocal elasticity theory, in micro and nanomaterials has received a considerable attention within the nanotechnology community. Tounsi *et al.* (2013) proposed a version of nonlocal elasticity theory which is employed to develop the thermal buckling properties of double-walled carbon nanotubes (DWCNTs) using nonlocal Timoshenko beam model. Besseghier *et al.* (2015) carried out the nonlinear vibration analysis of an embedded zigzag single-walled carbon nanotube based on nonlocal continuum theory. Aydogdu (2009) proposed a generalized nonlocal beam theory to study bending, buckling, and free vibration of nanobeams based on Eringen model using different beam theories. Pradhan and Murmu (2010) investigated the flap wise bending-vibration characteristics of a rotating nanocantilever by using Differential quadrature method (DQM). They noticed that small-scale effects play a significant role in the vibration response of a rotating nanocantilever. Civalek *et al.* (2010) presented a formulation of the equations of motion and bending of Euler-Bernoulli beam using the nonlocal elasticity theory for cantilever microtubules. The method of differential quadrature has been used for numerical modeling. Chemi *et al.* (2015) developed a chiral carbon nanotube model for the buckling analysis of DWCNTs. The size effect is taken into consideration using the Eringen's nonlocal elasticity theory.

In terms of vibration analysis of FGM beams with classical and non-classical boundary conditions there are a number of previous investigations on this topic. By using the Chebyshev collocation method, Sari and Butcher (2012) presented vibration analysis of non-rotating and rotating Timoshenko beams with damaged boundaries. Simsek (2010) developed different higher-order beam theories for vibration analysis of FG beams with various classical boundary conditions. Wattanasakulpong and Ungbhakorn (2014) predicted linear and nonlinear vibration analysis of elastically restrained ends FGM beams with porosities. They used the translational and rotational springs to simulate the non-classical boundary conditions for FGM beams with porosity. Shahba *et al.* (2011) presented free vibration and stability analysis of axially FG Timoshenko beams with both classical and non-classical boundary conditions. The governing equations of motion were then solved using a finite element approach.

Also, it is well-known that the effects of rotary inertia and shear deformation are neglected in the

Euler-Bernoulli beam theory (EBT). Due to this cause, the EBT always overestimates buckling load and natural frequency of free vibration and underestimates deflection. Moreover, in Timoshenko beam theory a shear correction factor is required to compensate for the difference between the actual stress state and the constant stress state. To avoid the use of shear correction factor and obtain better prediction of response of deep beam, many higher-order shear deformation theories have been developed such as the third-order shear deformation theory proposed (Hebali *et al.* 2014, Hamidi *et al.* 2015, Bennoun *et al.* 2016). In the FGM structures analysis area, Tounsi *et al.* (2015) utilized a simple and refined trigonometric higher-order beam theory to model the bending and vibration of functionally graded beams. Also, Belabed *et al.* (2014) used an efficient and simple higher order shear and normal deformation theory to investigate bending and free vibration analysis of functionally graded plates.

Nowadays, with the development of the material technology, FGMs have also been employed in MEMS/NEMS (Witvrouw and Mehta 2005, Bounouara *et al.* 2016). Actually, FGMs find increasing applications in micro- and nano-scale structures such as thin films in the form of shape memory alloys, atomic force microscopes (AFMs), micro sensors, micro piezo actuator and nano-motors. In all of these applications, the size effect plays major role which should be considered to study the mechanical behaviors of such small scale structures. Beams are the core structures widely used in MEMS, NEMS and AFMS with the order of microns or sub-microns, and their properties are closely related to their micro-structures. Thus, establishing an accurate model of FG nanobeams is a key issue for successful NEMS design. Asghari *et al.* (2010, 2011) studied the free vibration of the FGM Euler–Bernoulli microbeams, which has been extended to consider a size-dependent Timoshenko beam based on the modified couple stress theory. The dynamic characteristics of FG beam with power law material graduation in the axial or the transversal directions were examined by Alshorbagy *et al.* (2011). Sharabiani and Haeri Yazdi (2013) studied surface effects on nonlinear free vibration of functionally graded nanobeam within the framework of Euler-Bernoulli beam model on the basis of von Karman geometric nonlinearity. Hosseini-Hashemi and Nazemnezhad (2013) investigated nonlinear free vibration of simply supported Euler-Bernoulli FG nanobeams with considering surface effects and balance condition between the FG nanobeam bulk and its surfaces. The multiple scales method was used as an analytical solution for the nonlinear governing equation. Ke and Wang (2011) exploited the size effect on dynamic stability of functionally graded Timoshenko microbeams. The free vibration analysis of FG microbeams was presented by Ansari *et al.* (2011) based on the strain gradient Timoshenko beam theory. They also concluded that the value of gradient index plays an important role in the vibrational response of the FG microbeams of lower slenderness ratios. Employing modified couple stress theory the nonlinear free vibration of FG microbeams based on von-Karman geometric nonlinearity was presented by Ke *et al.* (2012). It was revealed that both the linear and nonlinear frequencies increase significantly when the thickness of the FGM microbeam was comparable to the material length scale parameter. Eltaher *et al.* (2012, 2013) presented a finite element formulation for free vibration analysis of FG nanobeams based on nonlocal Euler beam theory. They also exploited the size-dependent static-buckling behavior of functionally graded nanobeams on the basis of the nonlocal continuum model (2013). Recently, using nonlocal continuum theory, Mahmoud *et al.* (2015) investigated bending and buckling behaviors of size-dependent nanobeams made of functionally graded materials including the thickness stretching effect by Navier analytical method. More recently, Zemri *et al.* (2015) developed a nonlocal shear deformation beam theory for bending, buckling, and vibration of FG nanobeams using the nonlocal differential constitutive relations of Eringen.

It is found that most of the previous studies on vibration analysis of FG nanobeams have been conducted based on the ignorance of the non-classical boundary condition and different material composition effects. As a result, these studies cannot be utilized in order to thoroughly study the FG nanobeams under investigation. Therefore, there is strong scientific need to understand the vibration behavior of FG nanobeams in considering the effect of non-classical or non-ideal boundary conditions.

Motivated by this fact, in this study, vibration characteristics of FG nanobeams considering the effects of classical and non-classical boundary conditions is analyzed. Therefore, the translational and rotational springs are used to simulate the non-classical boundary conditions for FG nanobeams. A semi-analytical method called differential transformation method (DTM) is employed for vibration analysis of size-dependent FG nanobeams with three combinations of non-ideal boundary conditions for the first time. The superiority of the DTM is its simplicity and good precision and series expansion while it takes less time to solve polynomial series. It is different from the traditional high order Taylor's series method, which requires symbolic competition of the necessary derivatives of the data functions. The Taylor series method is computationally taken long time for large orders. With this method, it is possible to obtain highly accurate results or exact solutions for differential equations.

The material properties of FG nano beams are evaluated using the power law, sigmoid and Mori-Tanaka homogenization technique. Nonlocal Euler–Bernoulli beam model and Eringen's nonlocal elasticity theory are employed. Governing equations and different boundary conditions for the free vibration of a nonlocal FG beam have been derived via Hamilton's principle. These equations are solved using DTM and numerical solutions are obtained. The detailed mathematical derivations are presented while the emphasis is placed on investigating the effect of several parameters such as spring constant factors, different material compositions, mode number, various boundary conditions and small scale on vibration characteristics of FG nanobeams. Comparisons with the results from the existing literature are provided and the good agreement between the results of this article and those available in literature validated the presented approach. Numerical results are presented to serve as benchmarks for the application and the design of nanoelectronic and nano-drive devices, nano-oscillators, and nanosensors, in which nanobeams act as basic elements. They can also be useful as valuable sources for validating other approaches and approximate methods.

2. Material gradient of FG nano beams

Consider a FG nanobeam of length L and uniform thickness h in the unstressed reference configuration. The coordinate system for FG nanobeam with non-classical boundary conditions is shown in Fig. 1. The nanobeam is made of elastic and isotropic functionally graded material with

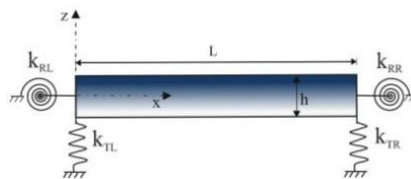


Fig. 1 Geometry and coordinates of E-E functionally graded nanobeam

properties varying smoothly in the z thickness direction only. It is assumed that bottom surface ($z=-h/2$) of FG nanobeam is pure metal (Al), whereas the top surface ($z=h/2$) is pure ceramics (Al_2O_3). Most researchers use the power-law, sigmoid and Mori-Tanaka scheme to describe the volume fractions of the FGM beams. Therefore, FG nano beams with power-law (P-FGM), Mori-Tanaka (MT-FGM) and sigmoid (S-FGM) function will be considered in this paper.

2.1 The material properties of P-FG nanobeams

One of the most favorable models for FGMs is the power-law model, in which material properties of FGMs are assumed to vary according to a power law about spatial coordinates. The effective material properties of the FG beam such as Young's modulus E_f , shear modulus G_f and mass density ρ_f are assumed to vary continuously in the thickness direction (z -axis direction) according to a power function of the volume fractions of the constituents. According to the rule of mixture, the effective material properties, P_f , can be expressed as Şimşek (2010)

$$P_f = P_c V_c + P_m V_m \quad (1)$$

Where P_m , P_c , V_m and V_c are the material properties and the volume fractions of the metal and the ceramic constituents related by

$$V_c + V_m = 1 \quad (2a)$$

The volume fraction of the ceramic constituent of the beam is assumed to be given by

$$V_c = \left(\frac{z}{h} + \frac{1}{2}\right)^p \quad (2b)$$

Here p is the non-negative variable parameter (power-law exponent) which determines the material distribution through the thickness of the beam and z is the distance from the mid-plane of the FG beam. The FG beam becomes a fully ceramic beam when p is set to be zero. Therefore, from Eqs. (1)-(2), the effective material properties of the FG nanobeam can be expressed as follows

$$\begin{aligned} E(z) &= (E_c - E_m) \left(\frac{z}{h} + \frac{1}{2}\right)^p + E_m \\ \rho(z) &= (\rho_c - \rho_m) \left(\frac{z}{h} + \frac{1}{2}\right)^p + \rho_m \end{aligned} \quad (3)$$

2.2 The material properties of MT-FG nanobeams

Additionally, in this study, Mori-Tanaka homogenization technique is also employed to model

Table 1 Material properties of FGM constituents Asghari *et al.* (2010)

| Material | | Young modulus [GPa] | Density [kg/m ³] | Poisson's ratio |
|----------|----------|---------------------|------------------------------|-----------------|
| Ceramic | Alumina | 380 | 3960 | 0.3 |
| Metal | Aluminum | 70 | 2702 | 0.3 |

the effective material properties of the FG nanobeams. According to Mori-Tanaka homogenization technique the local effective material properties of the FG nanobeam such as effective local bulk modulus K_e and shear modulus μ_e can be calculated by

$$\frac{K_e - K_m}{K_c - K_m} = \frac{V_c}{1 + V_m(K_c - K_m)/(K_m + 4\mu_m/3)} \quad (4a)$$

$$\frac{\mu_e - \mu_m}{\mu_c - \mu_m} = \frac{V_c}{1 + V_m(\mu_c - \mu_m)/[\mu_m + \mu_m(9K_m + 8\mu_m)/(6(K_m + 2\mu_m))]} \quad (4b)$$

However Poisson's ratio of the FG nanobeam is assumed to be constant. Therefore from Eq. (4), the effective Young's modulus (E) and mass density (ρ) based on Mori-Tanaka scheme can be expressed by

$$E(z) = \frac{9K_e\mu_e}{3K_e + \mu_e} \rho(z) = \rho_c V_c + \rho_m V_m \quad (5)$$

2.3 The material properties of S-FG nano beams

According to sigmoid distribution (S-FGM), the volume fractions of the metal and the ceramic constituents using two power-law functions which ensure smooth distribution of stresses are defined by

$$V_f^c(z) = 1 - \frac{1}{2} \left(\frac{h/2 - z}{h/2} \right)^p \quad \text{for } 0 \leq z \leq h/2$$

$$V_f^m(z) = \frac{1}{2} \left(\frac{h/2 + z}{h/2} \right)^p \quad \text{for } -h/2 \leq z \leq 0 \quad (6)$$

By using the rule of mixture, the material properties (P) of the S-FG nano beam can be calculated by

$$P(z) = V_f^c(z) P_c + (1 - V_f^c(z)) P_m \quad \text{for } 0 \leq z \leq h/2$$

$$P(z) = V_f^m(z) P_c + (1 - V_f^m(z)) P_m \quad \text{for } -h/2 \leq z \leq 0 \quad (7)$$

Where P , V_f^c , V_f^m are the material properties and the volume fractions of the ceramic and the metal constituents, respectively.

3. Theory and formulation

3.1 Kinematic relations

The equations of motion are derived based on the Euler-Bernoulli beam theory according to which the displacement field at any point of the beam can be written as

$$u_x(x, z, t) = u(x, t) - z \frac{\partial w(x, t)}{\partial x} \quad u_z(x, z, t) = w(x, t) \quad (8)$$

Where t is the time, u and w are displacement components of the mid-plane along x and z directions, respectively. Therefore, according to Euler–Bernoulli beam theory, every elements of strain tensor vanish except normal strain in the x -direction. Thus, the only nonzero strain is

$$\varepsilon_{xx} = \varepsilon_{xx}^0 - zk^0, \quad \varepsilon_{xx}^0 = \frac{\partial u(x, t)}{\partial x}, \quad k^0 = \frac{\partial^2 w(x, t)}{\partial x^2} \quad (9)$$

Where ε_{xx}^0 is the extensional strain and k^0 is the bending strain. Based on the Hamilton's principle, which states that, the motion of an elastic structure during the time interval $0 < t < t_2$ is such that the time integral of the total dynamics potential is extremum

$$\int_0^t \delta(U - T + W_{ext}) dt = 0 \quad (10)$$

Here U is strain energy of the system and $\delta U = \int_V \sigma_{ij} \delta \varepsilon_{ij} dV$, T is kinetic energy and W_{ext} is work done by external forces. The total strain energy for FG nanobeam can be expressed by taking into consideration effect of spring constants (induced by the non-classical boundary conditions) in addition to strain energy

$$\begin{aligned} \delta U = & \int_V (\sigma_{xx} \delta \varepsilon_{xx}) dV + K_{TL} w(0, t) \delta w(0, t) + K_{RL} \frac{\partial w(0, t)}{\partial x} \delta \left(\frac{\partial w(0, t)}{\partial x} \right) \\ & + K_{TR} w(L, t) \delta w(L, t) + K_{RR} \frac{\partial w(L, t)}{\partial x} \delta \left(\frac{\partial w(L, t)}{\partial x} \right) \end{aligned} \quad (11)$$

Where K_{RL} and K_{TL} are the corresponding rotational and translational spring constants at the left end, respectively. Similarly, K_{RR} and K_{TR} are the rotational and translational spring constants at the right end of FG nanobeam, respectively. Substituting Eq. (9) into Eq. (11) yields

$$\begin{aligned} \delta U = & \int_0^L (N (\delta \varepsilon_{xx}^0) - M (\delta k^0)) dx + K_{TL} w(0, t) \delta w(0, t) + K_{RL} \frac{\partial w(0, t)}{\partial x} \delta \left(\frac{\partial w(0, t)}{\partial x} \right) \\ & + K_{TR} w(L, t) \delta w(L, t) + K_{RR} \frac{\partial w(L, t)}{\partial x} \delta \left(\frac{\partial w(L, t)}{\partial x} \right) \end{aligned} \quad (12)$$

In which N and M are the axial force and bending moment respectively. These stress resultants used in Eq. (12) are defined as

$$N = \int_A \sigma_{xx} dA, \quad M = \int_A \sigma_{xx} z dA \quad (13)$$

The kinetic energy for Euler-Bernoulli beam is presented as well by

$$T = \frac{1}{2} \int_0^L \int_A \rho(z) \left(\left(\frac{\partial u_x}{\partial t} \right)^2 + \left(\frac{\partial u_z}{\partial t} \right)^2 \right) dA dx \quad (14)$$

Also the virtual kinetic energy can be expressed as

$$\delta T = \int_0^L \left[I_0 \left(\frac{\partial u}{\partial t} \frac{\partial \delta u}{\partial t} + \frac{\partial w}{\partial t} \frac{\partial \delta w}{\partial t} \right) - I_1 \left(\frac{\partial u}{\partial t} \frac{\partial^2 \delta w}{\partial t \partial x} + \frac{\partial \delta u}{\partial t} \frac{\partial^2 w}{\partial t \partial x} \right) + I_2 \frac{\partial^2 w}{\partial t \partial x} \frac{\partial^2 \delta w}{\partial t \partial x} \right] dx \quad (15)$$

Where (I_0, I_1, I_2) are the mass moments of inertias, defined as below

$$(I_0, I_1, I_2) = \int_A \rho(z) (1, z, z^2) dA \quad (16)$$

The first variation of external forces work of the beam can be written in the form

$$\delta W_{ext} = \int_0^L (f(x) \delta u + q(x) \delta w) dx \quad (17)$$

Where $f(x)$ and $q(x)$ are external axial and transverse loads distribution along length of beam, respectively. By Substituting Eqs. (12), (15) and (17) into Eq. (10) and setting the coefficients of δu , δw and $\delta \partial w / \partial x$ to zero, the following Euler-Lagrange equation can be obtained

$$\frac{\partial N}{\partial x} + f = I_0 \frac{\partial^2 u}{\partial t^2} - I_1 \frac{\partial^3 w}{\partial x \partial t^2} \quad (18a)$$

$$\frac{\partial^2 M}{\partial x^2} + q = I_0 \frac{\partial^2 w}{\partial t^2} + I_1 \frac{\partial^3 u}{\partial x \partial t^2} - I_2 \frac{\partial^4 w}{\partial x^2 \partial t^2} \quad (18b)$$

For simplification, the mass moment of inertia terms are assumed to be negligible and applied external axial load is set to zero for free vibration which results in a simplified version of Euler-Lagrange equation as

$$\frac{\partial N}{\partial x} = 0, \quad \frac{\partial^2 M}{\partial x^2} + q = I_0 \frac{\partial^2 w}{\partial t^2} + I_1 \frac{\partial^3 u}{\partial x \partial t^2} - I_2 \frac{\partial^4 w}{\partial x^2 \partial t^2} \quad (19)$$

Under the following boundary conditions, the relationship between bending moment and spring constants can be written as

$$-M - K_{RL} \frac{\partial w}{\partial x} = 0, \quad \frac{\partial M}{\partial x} - K_{TL} w = 0 \quad \text{at } x = 0 \quad (20a)$$

$$M - K_{RR} \frac{\partial w}{\partial x} = 0, \quad -\frac{\partial M}{\partial x} - K_{TR} w = 0 \quad \text{at } x = L \quad (20b)$$

3.2 The nonlocal elasticity model for FG nanobeam

Based on Eringen nonlocal elasticity model, the stress at a reference point x in a body is considered as a function of strains of all points in the near region. This assumption is agreement with experimental observations of atomic theory and lattice dynamics in phonon scattering in which for a homogeneous and isotropic elastic solid the nonlocal stress-tensor components σ_{ij} at any point x in the body can be expressed as

$$\sigma_{ij}(x) = \int_{\Omega} \alpha(|x' - x|, \tau) t_{ij}(x') d\Omega(x') \quad (21)$$

where $t_{ij}(x')$ are the components of the classical local stress tensor at point x which are related to the components of the linear strain tensor ε_{kl} by the conventional constitutive relations for a Hookean material, i.e.

$$t_{ij} = C_{ijkl} \varepsilon_{kl} \quad (22)$$

The meaning of Eq. (21) is that the nonlocal stress at point x is the weighted average of the local stress of all points in the neighborhood of x , the size of which is related to the nonlocal kernel $\alpha(|x' - x|, \tau)$. Here $|x' - x|$ is the Euclidean distance and τ is a constant given by

$$\tau = \frac{e_0 a}{l} \quad (23)$$

Which represents the ratio between a characteristic internal length, a (such as lattice parameter, C-C bond length and granular distance) and a characteristic external one, l (e.g., crack length, wavelength) through an adjusting constant, e_0 , dependent on each material. The magnitude of e_0 is determined experimentally or approximated by matching the dispersion curves of plane waves with those of atomic lattice dynamics. According to Eringen (1983) for a class of physically admissible kernel $\alpha(|x' - x|, \tau)$ it is possible to represent the integral constitutive relations given by Eq. (21) in an equivalent differential form as

$$(1 - (e_0 a)^2 \nabla^2) \sigma_{kl} = t_{kl} \quad (24)$$

As ∇^2 is the Laplacian operator. The parameter $e_0 a$ is the scale coefficient revealing the small scale effect on the responses of structures of nano size. The value of the small-scale parameter depends on boundary condition, chirality, mode shapes, number of walls, and the nature of motions (Tounsi *et al.* 2013, Besseghier *et al.* 2015). The parameter $e_0 = (\pi^2 - 4)^{1/2} / 2\pi \cong 0.39$ was given by Eringen (1983). The nonlocal parameter, $\mu = (e_0 a)^2$, is experimentally obtained for various materials; for instance, a conservative estimate of $\mu < 4 \text{ (nm)}^2$ for a single-walled carbon nanotube is proposed (Chemi *et al.* 2015). It is worthy to mention that this value is also chirality and size dependent, because the material properties of CNTs are widely acknowledged to be chirality dependent. For an elastic material in the one dimensional case, the nonlocal constitutive relations may be simplified as

$$\sigma(x) - (e_0 a)^2 \frac{\partial^2 \sigma(x)}{\partial x^2} = E \varepsilon(x) \quad (25)$$

Where σ and ε are the nonlocal stress and strain, respectively. E is the Young's modulus. For Euler-Bernoulli nonlocal FG beam, Eq. (25) can be written as

$$\sigma_{xx} - \mu \frac{\partial^2 \sigma_{xx}}{\partial x^2} = E(z) \varepsilon_{xx} \quad (26)$$

Where $(\mu = (e_0 a)^2)$. Integrating Eq. (26) over the beam's cross-section area, we obtain the force-strain and the moment-strain of the nonlocal Euler-Bernoulli FG beam theory can be

obtained as follows

$$N - \mu \frac{\partial^2 N}{\partial x^2} = A_{xx} \frac{\partial u}{\partial x} - B_{xx} \frac{\partial^2 w}{\partial x^2} \quad (27)$$

$$M - \mu \frac{\partial^2 M}{\partial x^2} = B_{xx} \frac{\partial u}{\partial x} - C_{xx} \frac{\partial^2 w}{\partial x^2} \quad (28)$$

In which the cross-sectional rigidities are defined as follows

$$(A_{xx}, B_{xx}, C_{xx}) = \int_A \frac{E(z)}{(1-\nu^2)} (1, z, z^2) dA \quad (29)$$

Where ν is the poisson's ratio. By using Eq. (19) it is concluded that N is a constant value throughout the beam; therefore, it can be expressed as

$$N = A_{xx} \frac{\partial u}{\partial x} - B_{xx} \frac{\partial^2 w}{\partial x^2} \quad (30)$$

Also the explicit relation of the nonlocal bending moment can be derived by substituting for the second derivative of M from Eq. (19) into Eq. (28) as follows

$$M = B_{xx} \frac{\partial u}{\partial x} - C_{xx} \frac{\partial^2 w}{\partial x^2} + \mu (I_0 \frac{\partial^2 w}{\partial t^2} + I_1 \frac{\partial^3 u}{\partial x \partial t^2} - I_2 \frac{\partial^4 w}{\partial x^2 \partial t^2} - q) \quad (31)$$

The nonlocal governing equations of Euler-Bernoulli FG nanobeam in terms of the displacement can be derived by combining for N and M from Eqs. (30) and (31), respectively, and substituting M into Eq. (19) as follows

$$\begin{aligned} & \frac{B_{xx}^2}{A_{xx}} \frac{\partial^4 w}{\partial x^4} - C_{xx} \frac{\partial^4 w}{\partial x^4} + \mu (I_0 \frac{\partial^4 w}{\partial t^2 \partial x^2} + \frac{B_{xx} I_1}{A_{xx}} \frac{\partial^6 w}{\partial t^2 \partial x^4} - I_2 \frac{\partial^6 w}{\partial t^2 \partial x^4} - \frac{\partial^2 q}{\partial x^2}) \\ & - I_0 \frac{\partial^2 w}{\partial t^2} - \frac{B_{xx} I_1}{A_{xx}} \frac{\partial^4 w}{\partial t^2 \partial x^2} + I_2 \frac{\partial^4 w}{\partial t^2 \partial x^2} + q = 0 \end{aligned} \quad (32)$$

4. Implementation of differential transform method

The differential transforms method provides an analytical solution procedure in the form of polynomials to solve ordinary and partial differential equations with small calculation errors and ability to solve nonlinear equations with boundary conditions value problems. Using DTM technique, the ordinary and partial differential equations can be transformed into algebraic equations, from which a closed-form series solution can be obtained easily. In this method, certain transformation rules are applied to both the governing differential equations of motion and the boundary conditions of the system in order to transform them into a set of algebraic equations. The solution of these algebraic equations gives the desired results of the problem. In this method, differential transformation of k_{th} derivative function $y(x)$ and differential inverse transformation of $Y(k)$ are respectively defined as follows

$$Y(k) = \frac{1}{k!} \left[\frac{d^k}{dx^k} y(x) \right]_{x=0} \tag{33}$$

$$y(x) = \sum_0^{\infty} x^k Y(k) \tag{34}$$

In which $y(x)$ is the original function and $Y(k)$ is the transformed function. Consequently from Eqs. (33) and (34) we obtain

$$y(x) = \sum_{k=0}^{\infty} \frac{x^k}{k!} \left[\frac{d^k}{dx^k} y(x) \right]_{x=0} \tag{35}$$

Eq. (35) reveals that the concept of the differential transformation is derived from Taylor’s series expansion. In real applications the function $y(x)$ in Eq. (35) can be written in a finite form as

$$y(x) = \sum_{k=0}^N x^k Y(k) \tag{36}$$

In this calculations $y(x) = \sum_{n+1}^{\infty} x^k Y(k)$ is small enough to be neglected, and N is determined by the convergence of the eigenvalues. From the definitions of DTM in Eqs. (33)-(35), the fundamental theorems of differential transforms method can be performed that are listed in Table 2 while Table 3 presents the differential transformation of conventional boundary conditions.

For harmonic vibration analysis, a sinusoidal variation of $w(x,t)$ with a circular natural frequency ω is assumed and the harmonic solution is approximated as

$$w(x,t) = w(x) e^{i\omega t} \tag{37}$$

Substituting Eq. (37) into Eq. (32), governing equation of motion can be rewritten as follows

$$\begin{aligned} & \frac{B_{xx}^2}{A_{xx}} \frac{\partial^4 w}{\partial x^4} - C_{xx} \frac{\partial^4 w}{\partial x^4} + \mu(-I_0 \omega^2 \frac{\partial^2 w}{\partial x^2} - \frac{B_{xx} I_1}{A_{xx}} \omega^2 \frac{\partial^4 w}{\partial x^4} + I_2 \omega^2 \frac{\partial^4 w}{\partial x^4} - \frac{\partial^2 q}{\partial x^2}) \\ & + I_0 \omega^2 w + \frac{B_{xx} I_1}{A_{xx}} \omega^2 \frac{\partial^2 w}{\partial x^2} - I_2 \omega^2 \frac{\partial^2 w}{\partial x^2} + q = 0 \end{aligned} \tag{38}$$

Table 2 Some of the transformation rules of the one-dimensional DTM

| Original function | Transformed function |
|--------------------------------|--|
| $f(x)=g(x)\pm h(x)$ | $F(K)=G(K)\pm H(K)$ |
| $f(x)=\lambda g(x)$ | $F(K)=\lambda G(K)$ |
| $f(x)=g(x)h(x)$ | $F(K) = \sum_{l=0}^K G(K-l)H(l)$ |
| $f(x) = \frac{d^n g(x)}{dx^n}$ | $F(K) = \frac{(k+n)!}{k!} G(K+n)$ |
| $f(x)=x^n$ | $F(K) = \delta(K-n) = \begin{cases} 1 & k = n \\ 0 & k \neq n \end{cases}$ |

Table 3 Transformed boundary conditions (B.C.) based on DTM

| $=0x$ Original B.C. | Transformed B.C. | $=Lx$ Original B.C. | Transformed B.C. |
|-----------------------------|------------------|------------------------|--|
| $f(0)=0$ | $F[0]=0$ | $f(L)=0$ | $\sum_{k=0}^{\infty} F[k] = 0$ |
| $\frac{df(0)}{dx} = 0$ | $F[1]=0$ | | $\sum_{k=0}^{\infty} k F[k] = 0$ |
| $\frac{d^2 f(0)}{dx^2} = 0$ | $F[2]=0$ | | $\sum_{k=0}^{\infty} k(k-1) F[k] = 0$ |
| $\frac{d^3 f(0)}{dx^3} = 0$ | $F[3]=0$ | | $\sum_{k=0}^{\infty} k(k-1)(k-2) F[k] = 0$ |

According to the basic transformation operations introduced in Table 2, the transformed form of the governing Eq. (38) around $x_0=0$ may be obtained as

$$\begin{aligned} & \left(\frac{B_{xx}^2}{A_{xx}} - C_{xx} \right) (k+1)(k+2)(k+3)(k+4)W[k+4] - I_0 \omega^2 (-W[k] + \mu(k+1)(k+2)W[k+2]) \\ & + \frac{B_{xx} I_1}{A_{xx}} \omega^2 (-\mu(k+1)(k+2)(k+3)(k+4)W[k+4] + (k+1)(k+2)W[k+2]) = 0 \quad (39) \\ & - I_2 \omega^2 (-\mu(k+1)(k+2)(k+3)(k+4)W[k+4] + (k+1)(k+2)W[k+2]) = 1 \end{aligned}$$

where $W[k]$ is the transformed function of w . Additionally, the differential transform method is applied to different pairs of classical boundary conditions at the ends of the FG nanobeam by using the theorems introduced in Table 3 and the following transformed classical boundary conditions are obtained.

Simply supported-Simply supported:

$$\begin{aligned} & W[0]=0, W[2]=0, W[1]=C_1, W[3]=C_2 \\ & \sum_{k=0}^{\infty} W[k] = 0, \sum_{k=0}^{\infty} k(k-1) W[k] = 0 \quad (40a) \end{aligned}$$

Clamped-Clamped:

$$\begin{aligned} & W[0]=0, W[1]=0, W[2]=C_1, W[3]=C_2 \\ & \sum_{k=0}^{\infty} W[k] = 0, \sum_{k=0}^{\infty} k W[k] = 0 \quad (40b) \end{aligned}$$

Clamped-Simply supported:

$$W[0]=0, W[1]=0, W[2]=C_1, W[3]=C_2$$

$$\sum_{k=0}^{\infty} W[k] = 0, \sum_{k=0}^{\infty} k(k-1)W[k] = 0 \quad (40c)$$

Clamped-Free:

$$W[0]=0, W[1]=0, W[2]=C_1, W[3]=C_2$$

$$\sum_{k=0}^{\infty} k(k-1)W[k] = 0, \sum_{k=0}^{\infty} k(k-1)(k-2)W[k] = 0 \quad (40d)$$

It is essential to investigate vibration analysis of FG nanobeams with non-classical boundary conditions consisting of translational and rotational springs. Damaged or non-ideal supports of FG beams can be modeled by using these springs (Wattanasakulpong and Ungbhakorn 2014). Therefore, the translational and rotational springs can be used to simulate the nonlocal FG beams with non-ideal conditions. By using Eq. (20), the transformed non-classical boundary conditions in terms of displacement and spring constants with various elastic supports can be written as:

Clamped-Elastic supported (C-E):

$$W[0]=0, W[1]=0, W[2]=C_1, W[3]=C_2$$

$$\sum_{k=0}^{\infty} \left(\frac{B_{xx}^2}{A_{xx}} - C_{xx} \right) k(k-1)W[k] - \sum_{k=0}^{\infty} K_{RR} k W[k] = 0 \quad (41a)$$

$$\sum_{k=0}^{\infty} \left(\frac{B_{xx}^2}{A_{xx}} - C_{xx} \right) k(k-1)(k-2)W[k] + \sum_{k=0}^{\infty} K_{TR} W[k] = 0$$

Simply-Elastic supported (S-E):

$$W[0]=0, W[2]=0, W[1]=C_1, W[3]=C_2$$

$$\sum_{k=0}^{\infty} \left(\frac{B_{xx}^2}{A_{xx}} - C_{xx} \right) k(k-1)W[k] - \sum_{k=0}^{\infty} K_{RR} k W[k] = 0 \quad (41b)$$

$$\sum_{k=0}^{\infty} \left(\frac{B_{xx}^2}{A_{xx}} - C_{xx} \right) k(k-1)(k-2)W[k] + \sum_{k=0}^{\infty} K_{TR} W[k] = 0$$

Elastic-Elastic supported (E-E):

$$W[0]=C_1, W[1]=C_2, W[2] = \frac{K_{RL}C_2}{2\left(\frac{B_{xx}^2}{A_{xx}} - C_{xx}\right)}, W[3] = \frac{K_{TL}C_1}{6\left(\frac{B_{xx}^2}{A_{xx}} - C_{xx}\right)} \quad (41c)$$

$$\sum_{k=0}^{\infty} \left(\frac{B_{xx}^2}{A_{xx}} - C_{xx} \right) k(k-1)W[k] - \sum_{k=0}^{\infty} K_{RR} k W[k] = 0$$

$$\sum_{k=0}^{\infty} \left(\frac{B_{xx}^2}{A_{xx}} - C_{xx} \right) k(k-1)(k-2)W[k] + \sum_{k=0}^{\infty} K_{TR} W[k] = 0$$

In this investigation, the spring constants which can be calculated in terms of moment of inertia (I) and Young's modulus from the following equations, $K_{TL} = \frac{\beta_{TL} E_m I}{L^3}$, $K_{RL} = \frac{\beta_{RL} E_m I}{L}$, $K_{TR} = \frac{\beta_{TR} E_m I}{L^3}$ and $K_{RR} = \frac{\beta_{RR} E_m I}{L}$, in which the corresponding values of β are the given parameters of spring constant factors. By using Eq. (39) with the transformed boundary conditions one arrives at the following eigenvalue problem

$$\begin{bmatrix} A_{11}(\omega) & A_{12}(\omega) \\ A_{21}(\omega) & A_{22}(\omega) \end{bmatrix} \begin{bmatrix} C_1 \\ C_2 \end{bmatrix} = 0 \quad (42a)$$

where $[C]$ correspond to the missing boundary conditions at $x=0$. For the non-trivial solutions of Eq. (42a), it is necessary that the determinant of the coefficient matrix is equal to zero

$$\begin{vmatrix} A_{11}(\omega) & A_{12}(\omega) \\ A_{21}(\omega) & A_{22}(\omega) \end{vmatrix} = 0 \quad (42b)$$

Solution of Eq. (42b) is simply a polynomial root finding problem. In the present study, the Newton-Raphson method is used to solve the governing equation of the non-dimensional natural frequencies. Solving Eq. (42b), the i^{th} estimated eigenvalue for n^{th} iteration ($\omega = \omega_i^{(n)}$) may be obtained and the total number of iterations is related to the accuracy of calculations which can be determined by the following equation

$$\left| \omega_i^{(n)} - \omega_i^{(n-1)} \right| < \varepsilon \quad (43)$$

In this study $\varepsilon=0.0001$ considered in procedure of finding eigenvalues which results in 4 digit precision in estimated eigenvalues. Further a Matlab program has been developed according to DTM rule stated above, in order to find eigenvalues. As mentioned before, DT method implies an iterative procedure to obtain the high-order Taylor series solution of differential equations. The Taylor series method requires a long computational time for large orders, whereas one advantage of employing DTM in solving differential equations is a fast convergence rate and a small calculation error.

5. Numerical results and discussions

Through this section, a numerical testing of the procedure as well as parametric studies are performed in order to establish the validity and usefulness of the DTM approach. The effect of spring constant factors, different material distribution, nonlocality effect and various boundary conditions on the natural frequencies of the FG nanobeam will be figured out. The nonlocal FG beams with classical boundary conditions supported by four different combinations of clamped

(C), simply-supported (S) and free (F) conditions at $x=0$; L are considered in the following: simply-supported/simply-supported, clamped/simply-supported, clamped/clamped, and clamped/free.

Additionally, different combinations of non-ideal boundary conditions for FG nanobeams with elastic (E) supports consisting of rotational and translational springs are presented in this section. Each combination will be shortly indicated by a two-letter notation corresponding to edge conditions at $x=0$ and $x=L$. For example, C-E stands for a nonlocal FG beam with clamped edge at $x=0$ and elastic supported edge at $x=L$. The functionally graded nanobeam is composed of steel and ceramic where its properties are given in Table 1. The bottom surface of the FG nanobeam is Aluminum (Al), whereas the top surface of the beam is Alumina (Al_2O_3). The beam geometry has the following dimensions: L (length)=10,000 nm, b (width)=1000 nm and h (thickness)=100 nm. Relation described in Eq. (44) is performed in order to calculate the non-dimensional natural frequencies

$$\bar{\omega} = \omega L^2 / h \sqrt{\rho_m / E_m} \tag{44}$$

While $I=bh^3/12$ is the moment of inertia of the cross section of the beam.

Table 4 shows the convergence study of DTM for first three natural frequencies of nanobeam with various gradient indexes and classical boundary conditions. It is found that in DTM after a certain number of iterations eigenvalues converged to a value with good precision. From results of Table 4, high convergence rate of the method may be easily observed and it may be deduced that the third natural frequency of FG nanobeam with $p=0.5$ converged after 39 iterations with 4 digit precision while the first and second natural frequencies converged after 21 and 29 iterations respectively. To evaluate accuracy of the natural frequencies predicted by the present method, the non-dimensional natural frequencies of C-C functionally graded nanobeam with various nonlocal parameters and gradient indexes previously analyzed by finite element method are reexamined.

Tables 5 compares the results of the present study and the results presented by Eltahir *et al.* (2012) which has been obtained by finite element method for FG nanobeam with different nonlocal parameters (varying from 0 to 3). The reliability of the presented method and procedure for FG nanobeam may be concluded from Table 5; where the results are in an excellent agreement

Table 4 Convergence study of the P-FG nanobeam for the first three natural frequencies ($L/h=5$, $p=0.5$, $\mu=1$ nm)

| k | C-C | | | C-S | | | S-S | | | C-F | | |
|-----|------------------|------------------|------------------|------------------|------------------|------------------|------------------|------------------|------------------|------------------|------------------|------------------|
| | $\bar{\omega}_1$ | $\bar{\omega}_2$ | $\bar{\omega}_3$ |
| 11 | 9.3578 | - | - | 6.6686 | - | - | 4.3944 | - | - | 1.6724 | - | - |
| 15 | 9.7320 | - | - | 6.7697 | - | - | 4.3852 | - | - | 1.6725 | 9.6255 | - |
| 19 | 9.7461 | - | - | 6.7715 | - | - | 4.3852 | 14.8725 | - | 1.6725 | 9.5344 | - |
| 23 | 9.7462 | 22.1958 | - | 6.7715 | 18.4231 | - | 4.3852 | 14.8955 | - | 1.6725 | 9.5333 | 21.9000 |
| 27 | 9.7462 | 22.1466 | - | 6.7715 | 18.4149 | - | 4.3852 | 14.8957 | 27.0098 | 1.6725 | 9.5333 | 22.1847 |
| 31 | 9.7462 | 22.1460 | 34.2074 | 6.7715 | 18.4149 | 30.6187 | 4.3852 | 14.8957 | 26.9683 | 1.6725 | 9.5333 | 22.1906 |
| 35 | 9.7462 | 22.1460 | 34.3196 | 6.7715 | 18.4149 | 30.6377 | 4.3852 | 14.8957 | 26.9678 | 1.6725 | 9.5333 | 22.1906 |
| 39 | 9.7462 | 22.1460 | 34.3215 | 6.7715 | 18.4149 | 30.6379 | 4.3852 | 14.8957 | 26.9678 | 1.6725 | 9.5333 | 22.1906 |
| 43 | 9.7462 | 22.1460 | 34.3215 | 6.7715 | 18.4149 | 30.6379 | 4.3852 | 14.8957 | 26.9678 | 1.6725 | 9.5333 | 22.1906 |

Table 5 Comparison of the non-dimensional fundamental frequency for a P-FG nanobeam with various gradient indexes and nonlocal parameters with C-C boundary conditions ($L/h=100$, $K_{TL}=K_{TR}\rightarrow\infty$, $K_{RL}=K_{RR}\rightarrow\infty$)

| μ | $p=0$ | | $p=0.5$ | | $p=1$ | | $p=5$ | | $p=10$ | |
|-------|-------------------------------------|----------------|-------------------------------------|----------------|-------------------------------------|----------------|-------------------------------------|----------------|-------------------------------------|----------------|
| | FEM Eltaher <i>et al.</i> (2012) | Present DTM |
| 0 | 22.3744 | 22.3733 | 17.5613 | 17.5602 | 15.8612 | 15.8600 | 13.4733 | 13.4724 | 12.8698 | 12.8691 |
| 1 | 21.1096 | 21.1086 | 16.5686 | 16.5676 | 14.9645 | 14.9635 | 12.7116 | 12.7109 | 12.1423 | 12.1417 |
| 2 | 20.0330 | 20.0321 | 15.7235 | 15.7227 | 14.2013 | 14.2004 | 12.0633 | 12.0626 | 11.5230 | 11.5225 |
| 3 | 19.1028 | 19.1020 | 14.9934 | 14.9926 | 13.5419 | 13.5410 | 11.5032 | 11.5026 | 10.9880 | 10.9875 |

Table 6 Classical boundary conditions and material graduation effect on first dimensionless frequency of a FG nanobeam with different non-locality parameters ($L/h=5$)

| Beam | μ | C-C | | | C-S | | | S-S | | | C-F | | |
|--------|-------|---------|--------|--------|---------|--------|--------|---------|--------|--------|---------|--------|--------|
| | | $p=0.5$ | $p=1$ | $p=5$ |
| P-FGM | | 10.3804 | 9.3859 | 8.1474 | 7.1622 | 6.4761 | 5.6218 | 4.5965 | 4.1560 | 3.6083 | 1.6656 | 1.5057 | 1.3084 |
| S-FGM | 0 | 9.8211 | 9.3859 | 8.4257 | 6.7765 | 6.4761 | 5.8132 | 4.3491 | 4.1560 | 3.7302 | 1.5763 | 1.5057 | 1.3504 |
| MT-FGM | | 9.0957 | 8.3955 | 7.6932 | 6.2758 | 5.7926 | 5.3085 | 4.0275 | 3.7174 | 3.4073 | 1.4591 | 1.3466 | 1.2357 |
| P-FGM | | 9.2139 | 8.3319 | 7.2294 | 6.4377 | 5.8210 | 5.0526 | 4.2006 | 3.7981 | 3.2975 | 1.6796 | 1.5184 | 1.3194 |
| S-FGM | 2 | 8.7165 | 8.3319 | 7.4824 | 6.0907 | 5.8210 | 5.2258 | 3.9745 | 3.7981 | 3.4089 | 1.5896 | 1.5184 | 1.3618 |
| MT-FGM | | 8.0743 | 7.4532 | 6.8258 | 5.6410 | 5.2069 | 4.7708 | 3.6806 | 3.3972 | 3.1138 | 1.4714 | 1.3580 | 1.2461 |
| P-FGM | | 8.3646 | 7.5642 | 6.5616 | 5.8941 | 5.3296 | 4.6256 | 3.8920 | 3.5191 | 3.0552 | 1.6944 | 1.5318 | 1.3310 |
| S-FGM | 4 | 7.9125 | 7.5642 | 6.7947 | 5.5763 | 5.3296 | 4.7850 | 3.6825 | 3.5191 | 3.1585 | 1.6036 | 1.5318 | 1.3738 |
| MT-FGM | | 7.3305 | 6.7668 | 6.1948 | 5.1648 | 4.7673 | 4.3676 | 3.4102 | 3.1476 | 2.8851 | 1.4844 | 1.3700 | 1.2571 |

Table 7 Comparison of the non-dimensional fundamental frequency for a P-FGM beam with various gradient indexes and spring constant factors with E-E boundary conditions ($L/h=30$, $\beta_{TL}=\beta_{TR}=\beta_{RL}=\beta_{RR}=\beta$)

| β | $p=0.5$ | | $p=1$ | | $p=2$ | | $p=5$ | |
|---------|--|----------------|--|----------------|--|----------------|--|----------------|
| | Wattanasakulpong and Ungbhakorn (2014) | Present DTM |
| 1 | 0.373 | 0.373064 | 0.384 | 0.384412 | 0.397 | 0.396861 | 0.411 | 0.410697 |
| 10 | 1.168 | 1.168100 | 1.202 | 1.201867 | 1.239 | 1.238884 | 1.281 | 1.280603 |
| 10^2 | 3.551 | 3.550701 | 3.618 | 3.618353 | 3.686 | 3.686041 | 3.773 | 3.772986 |
| 10^3 | 8.382 | 8.381776 | 8.020 | 8.020096 | 7.653 | 7.652800 | 7.476 | 7.475708 |
| 10^4 | 10.750 | 10.749748 | 9.789 | 9.789215 | 8.981 | 8.980804 | 8.576 | 8.576036 |
| 10^5 | 11.060 | 11.059846 | 10.006 | 10.006022 | 9.136 | 9.135825 | 8.701 | 8.701138 |

as values of non-dimensional fundamental frequency are consistent with presented analytical solution up to 4 digits.

In order to investigate the effects of different boundary conditions on FG nanobeam vibration characteristics, the non-dimensional frequencies of non-local FG beams with different edge conditions (C-C, C-S, S-S and C-F) are tabulated in Table 6, which figures out the effect of nonlocal parameter (varying from 0 to 4), gradient index (varying from 0.5 to 5) and different material compositions (P-FGM, S-FGM and MT-FGM) for $L/h=5$ on the natural frequency characteristics of FG nanobeam. As seen in table, by fixing the nonlocal parameter and varying the material distribution parameter results decreasing in the fundamental frequencies, due to increasing in ceramics phase constituent, and hence, stiffness of the beam. On the other hand, it is revealed that the dimensionless natural frequencies decrease with an increase in material gradient index due to increasing in stiffness of the beam because of increasing in ceramic's phase constituent. However, the increasing of nonlocal parameter causes the decreasing in fundamental frequency, at a constant material graduation index. For clamped free beams, by fixing the material distribution parameter and increasing the nonlocal parameter results in increasing the fundamental frequencies. Also, as it is expected, a beam with stiffer edges; i.e., C-C and C-S, respectively shows higher natural frequencies than those of others boundary condition.

The fundamental frequency parameter as a function of power law indexes is presented in Fig. 2 for the P-FG nanobeams supported by different classical boundary conditions and nonlocal parameters. Similarly, the variation of the first dimensionless frequency of the S-FG nanobeam with material graduation and nonlocality parameters for different classical boundary conditions are depicted in Fig. 3. Observing these two figures, it is easily deduced for a FG nanobeam that, an increase in nonlocal scale parameter and gradient indexes gives rise to a decrease in the first dimensionless natural frequency for all boundary conditions. Also It can be observed that, the first frequency reduce with high rate where the power exponent in range from 0 to 2 than that where power exponent in range between 2 and 10. Fig. 4 displays the variations of the first dimensionless natural frequency of the P-FG nanobeam with respect to gradient indexes for different values of nonlocal parameters and classical boundary conditions ($L/h=5$). Similar to the case of classical

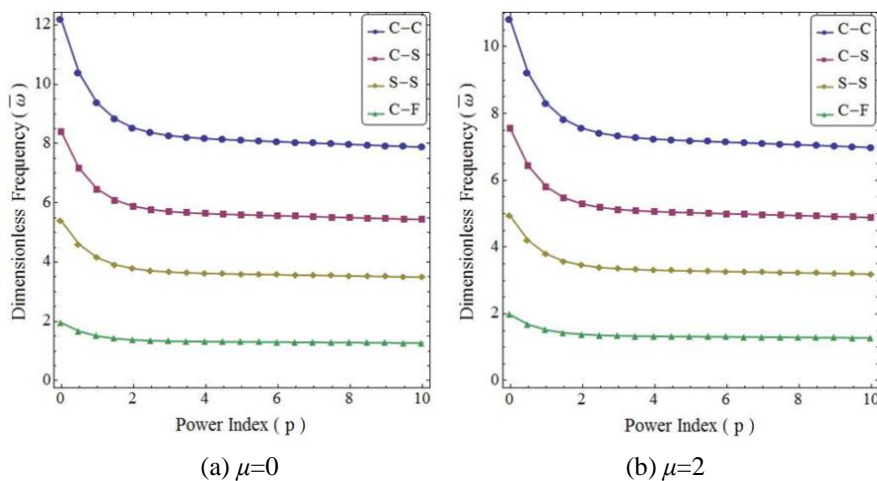


Fig. 2 Variations of the first dimensionless natural frequency of the P-FG nanobeam with respect to material graduation for different classical boundary conditions and nonlocal parameters ($L/h=5$)

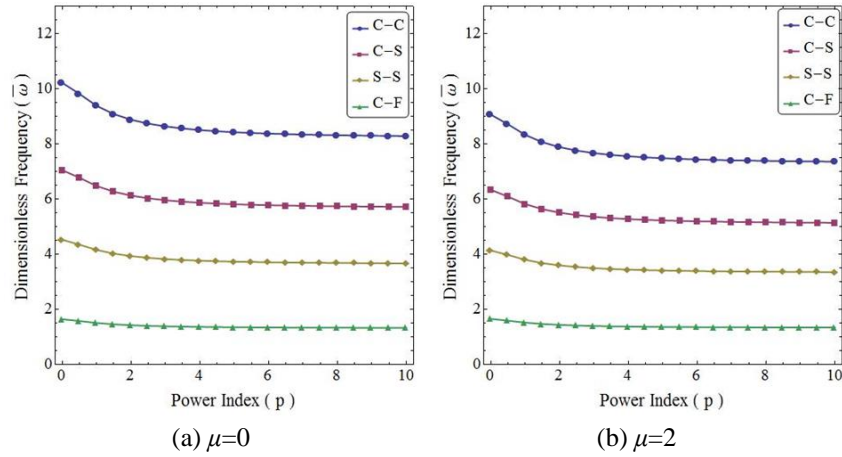


Fig. 3 Variations of the first dimensionless natural frequency of the S-FG nanobeam with respect to material gradation for different classical boundary conditions and nonlocal parameters ($L/h=5$)

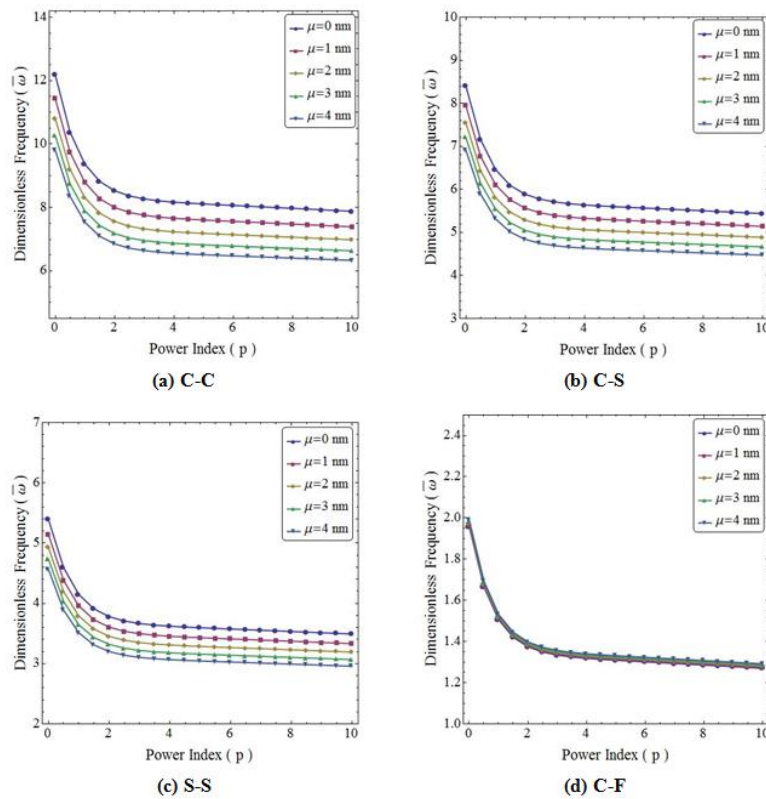


Fig. 4 The variation of the first dimensionless frequency of P-FG nanobeam with material gradation and non-locality parameters for various classical boundary conditions ($L/h=5$)

boundary condition, to demonstrate the correctness of present study the results for FGM beam with non-classical boundaries are compared with the results available in the literature.

Table 8 Effect of material in homogeneity on first three dimensionless frequencies of a FG nanobeam with different nonlocal parameters and non-classical boundary conditions ($\beta_{TL}=\beta_{TR}=\beta_{RL}=\beta_{RR}=10^3, L/h=20, p=2$)

| μ | $\bar{\omega}_i$ | P-FGM | | | S-FGM | | | MT-FGM | | |
|-------|------------------|---------------------|---------|---------|---------|---------|---------|---------|---------|---------|
| | | Boundary conditions | | | | | | | | |
| | | E-E | S-E | C-E | E-E | S-E | C-E | E-E | S-E | C-E |
| 0 | $i=1$ | 7.6528 | 5.8749 | 8.2728 | 7.7464 | 6.0247 | 8.4448 | 7.2930 | 5.5308 | 7.8205 |
| | $i=2$ | 15.8556 | 15.9679 | 18.7204 | 15.6915 | 16.0445 | 18.7955 | 15.4697 | 15.3393 | 18.0197 |
| | $i=3$ | 25.0750 | 29.0858 | 33.6715 | 25.0049 | 29.5913 | 34.4256 | 24.3569 | 27.6988 | 31.9006 |
| 2 | $i=1$ | 7.2076 | 5.3908 | 7.6395 | 7.3326 | 5.5419 | 7.8294 | 6.8350 | 5.0637 | 7.1951 |
| | $i=2$ | 13.8896 | 13.1971 | 15.4290 | 13.8559 | 13.3792 | 15.5702 | 13.4243 | 12.5509 | 14.7474 |
| | $i=3$ | 19.5272 | 20.2668 | 22.6398 | 19.4524 | 20.5073 | 23.0232 | 18.9670 | 19.3910 | 21.5808 |
| 4 | $i=1$ | 6.7992 | 4.9999 | 7.1063 | 6.9446 | 5.1484 | 7.3032 | 6.4235 | 4.6896 | 6.6761 |
| | $i=2$ | 12.3908 | 11.4364 | 13.3794 | 12.4454 | 11.6693 | 13.5762 | 11.8851 | 10.8078 | 12.7080 |
| | $i=3$ | 16.9425 | 16.8567 | 18.6297 | 16.8783 | 17.0265 | 18.8574 | 16.4303 | 16.1198 | 17.8250 |

Table 9 Material gradation and spring constant factor effect on first dimensionless frequency of an E-E FG nanobeam with different non-locality parameters ($L/h=20$)

| Beam | μ | $\beta_{TL}=\beta_{TR}=\beta_{RL}=\beta_{RR}$ | | | | | | | | | | | |
|--------|-------|---|--------|--------|---------|--------|--------|---------|--------|--------|-----------|--------|--------|
| | | 10 | | | 10^2 | | | 10^3 | | | 10^{24} | | |
| | | $p=0.5$ | $p=1$ | $p=5$ | $p=0.5$ | $p=1$ | $p=5$ | $p=0.5$ | $p=1$ | $p=5$ | $p=0.5$ | $p=1$ | $p=5$ |
| P-FGM | 0 | 1.1681 | 1.2018 | 1.2806 | 3.5507 | 3.6183 | 3.7729 | 8.3817 | 8.0201 | 7.4757 | 10.7497 | 9.7892 | 8.5760 |
| S-FGM | | 1.2027 | 1.2018 | 1.1996 | 3.6342 | 3.6183 | 3.5749 | 8.2406 | 8.0201 | 7.4838 | 10.2238 | 9.7892 | 8.8216 |
| MT-FGM | | 1.1657 | 1.1995 | 1.2790 | 3.5092 | 3.5736 | 3.7395 | 7.7746 | 7.4696 | 7.1712 | 9.4866 | 8.7975 | 8.1139 |
| P-FGM | 2 | 1.1658 | 1.1992 | 1.2774 | 3.5358 | 3.6007 | 3.7472 | 8.0455 | 7.6233 | 6.9992 | 9.7215 | 8.8315 | 7.7152 |
| S-FGM | | 1.2002 | 1.1992 | 1.1968 | 3.6175 | 3.6007 | 3.5544 | 7.8598 | 7.6233 | 7.0565 | 9.2306 | 8.8315 | 7.9462 |
| MT-FGM | | 1.1631 | 1.1967 | 1.2757 | 3.4921 | 3.5530 | 3.7110 | 7.3895 | 7.0415 | 6.6885 | 8.5585 | 7.9240 | 7.2951 |
| P-FGM | 4 | 1.1635 | 1.1966 | 1.2742 | 3.5207 | 3.5825 | 3.7202 | 7.7114 | 7.2447 | 6.5729 | 8.9247 | 8.0964 | 7.0616 |
| S-FGM | | 1.1977 | 1.1966 | 1.1940 | 3.6003 | 3.5825 | 3.5331 | 7.4912 | 7.2447 | 6.6625 | 8.4659 | 8.0964 | 7.2783 |
| MT-FGM | | 1.1606 | 1.1939 | 1.2724 | 3.4744 | 3.5316 | 3.6809 | 7.0222 | 6.6472 | 6.2637 | 7.8460 | 7.2577 | 6.6748 |

Table 7 compares the semi-analytical results of the present study and the results obtained for the FGM beam with various constituent volume fraction exponents and spring constant factors presented by Wattanasakulpong and Ungbhakorn (2014) which have been obtained by using Lagrange’s equations. One may clearly notice here that the fundamental frequency parameters obtained in the present investigation are in approximately close enough to the results provided in this literature and thus validates the proposed method of solution.

After extensive validation of the present formulation for FGM beams, the effects of different parameters such as spring constant factors, nonlocality parameter, different material models and gradient index on the vibration of FG nanobeams which are supported by different non-ideal boundary conditions including translational and rotational springs are investigated.

Table 8 shows the variation of first three dimensionless frequencies of P-FGM, S-FGM and

MT-FGM beams having $p=2$ with different non-classical boundary conditions and non-local parameter. It can be concluded from the results of the table that increasing the nonlocality parameter yields the reduction in dimensionless frequencies for every material graduation. Additionally, as it is expected in this Table, the nonlocal FG beams with clamped support at left end and elastic support at another end (C-E) have larger natural frequencies than those of E-E and S-E functionally graded nanobeams.

In Table 9, a comparison between dimensionless natural frequencies of the FG nanobeams with elastic supported at both ends, defined as E–E beams subjected to different material compositions (P-FGM, S-FGM and MT-FGM) and various spring constant factors are presented for various values of the gradient index ($p=0.5,1,5$) and nonlocal parameters ($\mu=0,2,4$) for $L/h=20$ based on DT method. It can be observed that the dimensionless natural frequencies increase by increasing spring constant factors and it can be stated that spring constant has a notable effect on the natural frequencies. It can also be seen that the present results for P-FGM and S-FGM models are identical for a FG nanobeam with $p=1$.

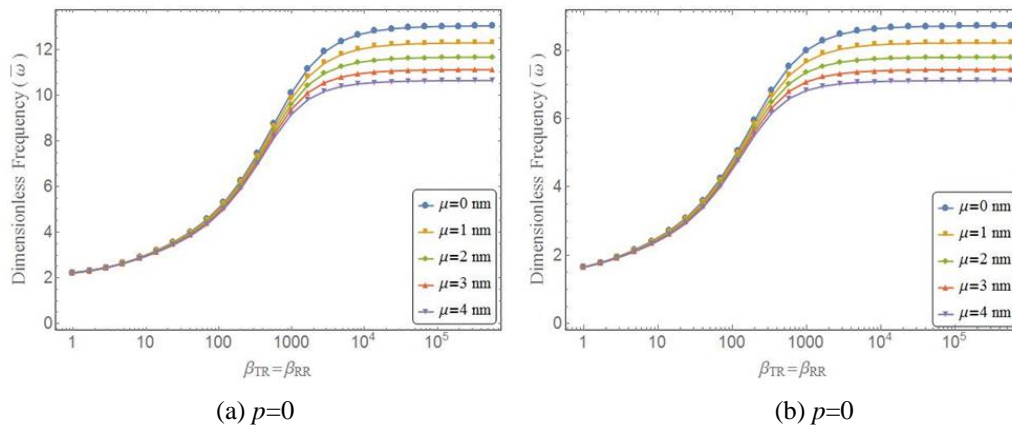


Fig. 5 The variation of the first dimensionless frequency of P-FG nanobeam with spring constant factor and nonlocality parameters for different gradient indexes with C-E boundary conditions ($L/h=20$)

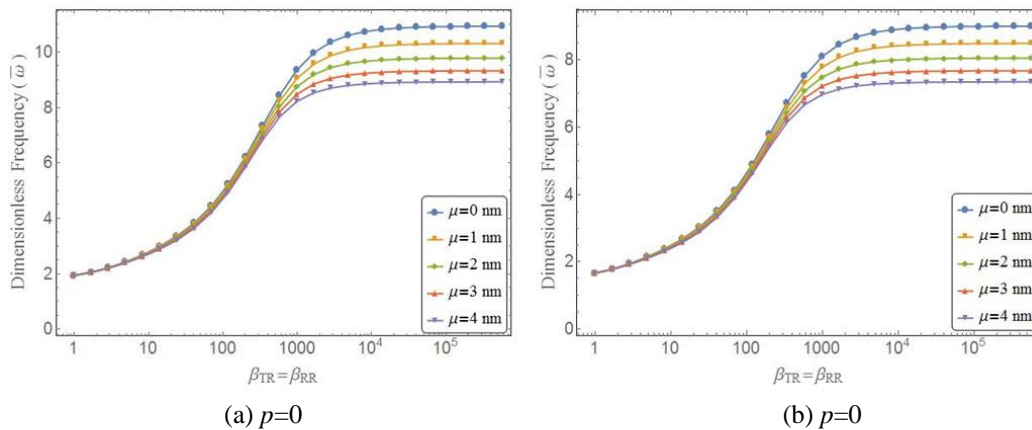


Fig. 6 The variation of the first dimensionless frequency of S-FG nanobeam with spring constant factor and non-locality parameters for different gradient indexes with C-E boundary conditions ($L/h=20$)

Table 10 Material graduation and spring constant factor effect on first dimensionless frequency of a C-E FG nanobeam with different non-locality parameters ($L/h=20$)

| Beam | μ | $\beta_{TR}=\beta_{RR}$ | | | | | | | | | | | |
|--------|-------|-------------------------|--------|--------|---------|--------|--------|---------|--------|--------|---------|--------|--------|
| | | 10 | | | 10^2 | | | 10^3 | | | 10^4 | | |
| | | $p=0.5$ | $p=1$ | $p=5$ | $p=0.5$ | $p=1$ | $p=5$ | $p=0.5$ | $p=1$ | $p=5$ | $p=0.5$ | $p=1$ | $p=5$ |
| P-FGM | | 2.7782 | 2.6483 | 2.5115 | 4.8933 | 4.8079 | 4.7826 | 9.3695 | 8.8065 | 8.0037 | 10.9174 | 9.9072 | 8.6446 |
| S-FGM | 0 | 2.7212 | 2.6483 | 2.4850 | 4.8877 | 4.8079 | 4.6277 | 9.1040 | 8.8065 | 8.1050 | 10.3586 | 9.9072 | 8.9074 |
| MT-FGM | | 2.5673 | 2.4809 | 2.4323 | 4.6619 | 4.6231 | 4.6882 | 8.5360 | 8.0869 | 7.6311 | 9.6007 | 8.8826 | 8.1718 |
| P-FGM | | 2.7400 | 2.6050 | 2.4612 | 4.7566 | 4.6705 | 4.6391 | 8.7924 | 8.1929 | 7.3583 | 9.8221 | 8.9018 | 7.7557 |
| S-FGM | 2 | 2.6791 | 2.6050 | 2.4394 | 4.7491 | 4.6705 | 4.4925 | 8.4945 | 8.1929 | 7.4913 | 9.3111 | 8.9018 | 7.9971 |
| MT-FGM | | 2.5253 | 2.4353 | 2.3814 | 4.5286 | 4.4879 | 4.5446 | 7.9407 | 7.4731 | 6.9965 | 8.6264 | 7.9744 | 7.3292 |
| P-FGM | | 2.7036 | 2.5641 | 2.4139 | 4.6302 | 4.5436 | 4.5064 | 8.2767 | 7.6612 | 6.8242 | 8.9904 | 8.1421 | 7.0879 |
| S-FGM | 4 | 2.6392 | 2.5641 | 2.3964 | 4.6210 | 4.5436 | 4.3676 | 7.9607 | 7.6612 | 6.9727 | 8.5183 | 8.1421 | 7.3113 |
| MT-FGM | | 2.4855 | 2.3922 | 2.3336 | 4.4055 | 4.3631 | 4.4118 | 7.4251 | 6.9549 | 6.4771 | 7.8902 | 7.2904 | 6.6969 |

Table 11 Material graduation and spring constant factor effect on first dimensionless frequency of a S-E FG nanobeam with different non-locality parameters ($L/h=20$)

| Beam | μ | $\beta_{TR}=\beta_{RR}$ | | | | | | | | | | | |
|--------|-------|-------------------------|--------|--------|---------|--------|--------|---------|--------|--------|---------|--------|--------|
| | | 10 | | | 10^2 | | | 10^3 | | | 10^4 | | |
| | | $p=0.5$ | $p=1$ | $p=5$ | $p=0.5$ | $p=1$ | $p=5$ | $p=0.5$ | $p=1$ | $p=5$ | $p=0.5$ | $p=1$ | $p=5$ |
| P-FGM | | 1.5814 | 1.5697 | 1.5806 | 3.6788 | 3.6655 | 3.6845 | 6.7898 | 6.3092 | 5.6561 | 7.5575 | 6.8508 | 5.9706 |
| S-FGM | 0 | 1.5908 | 1.5697 | 1.5207 | 3.7105 | 3.6655 | 3.5539 | 6.5468 | 6.3092 | 5.7613 | 7.1654 | 6.8508 | 6.1552 |
| MT-FGM | | 1.5221 | 1.5194 | 1.5551 | 3.5544 | 3.5508 | 3.6129 | 6.1149 | 5.7474 | 5.3772 | 6.6389 | 6.1380 | 5.6427 |
| P-FGM | | 1.5556 | 1.5415 | 1.5483 | 3.5757 | 3.5559 | 3.5575 | 6.2967 | 5.8164 | 5.1761 | 6.8305 | 6.1873 | 5.3878 |
| S-FGM | 2 | 1.5630 | 1.5415 | 1.4913 | 3.6022 | 3.5559 | 3.4402 | 6.0472 | 5.8164 | 5.2895 | 6.4729 | 6.1873 | 5.5565 |
| MT-FGM | | 1.4947 | 1.4900 | 1.5224 | 3.4481 | 3.4370 | 3.4821 | 5.6371 | 5.2761 | 4.9129 | 5.9959 | 5.5408 | 5.0909 |
| P-FGM | | 1.5310 | 1.5146 | 1.5178 | 3.4798 | 3.4539 | 3.4393 | 5.8825 | 5.4115 | 4.7923 | 6.2752 | 5.6819 | 4.9451 |
| S-FGM | 4 | 1.5366 | 1.5146 | 1.4635 | 3.5015 | 3.4539 | 3.3344 | 5.6337 | 5.4115 | 4.9076 | 5.9449 | 5.6819 | 5.1012 |
| MT-FGM | | 1.4687 | 1.4622 | 1.4916 | 3.3491 | 3.3311 | 3.3606 | 5.2445 | 4.8949 | 4.5439 | 5.5061 | 5.0867 | 4.6722 |

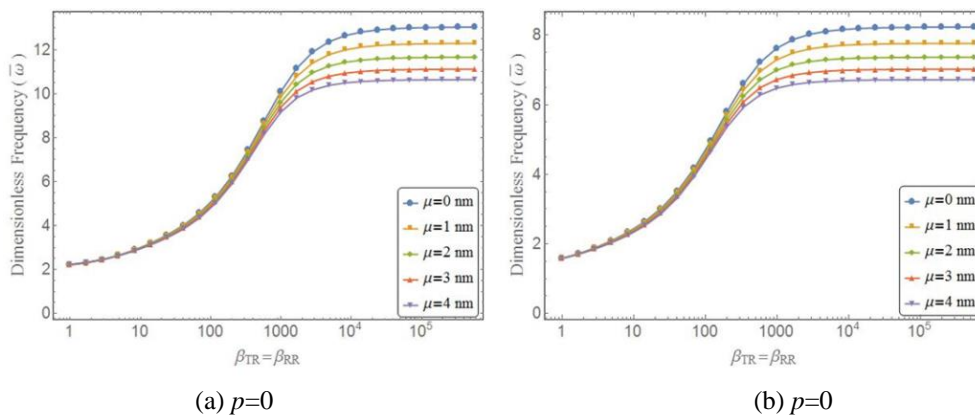


Fig. 7 The variation of the first dimensionless frequency of MT-FG nanobeam with spring constant factor and non-locality parameters for different gradient indexes with C-E boundary conditions ($L/h=20$)

In addition, it can be concluded from the results of this table that an increase in nonlocal scale parameter gives rise to a decrement in the first dimensionless natural frequencies. Variations of the first dimensionless natural frequencies of the C-E nonlocal FG beams with respect to spring constant factors for different values of nonlocal parameters and gradient indexes with P-FG, S-FG and MT-FG distributions are depicted in Figs. 5, 6 and 7, respectively.

It is seen from the figures that the fundamental frequency of FG nanobeam decreases with the increase of nonlocality parameters and power exponent. This is due to the reduction in total stiffness of the beam. One important observation within the range of spring constant factors in the range of the spring stiffness from 10^0 to 10^3 , it can be concluded there are slight differences in value of the frequency results of FG beam for every value of μ .

Also, it is seen that the FG nanobeams with lower value of spring constant usually provide lower values of the frequency results. Moreover, the variation of the first dimensionless frequency of C-E FG nanobeam with spring constant factors for different material compositions and small scale parameters are illustrated in Figs. 8-10.

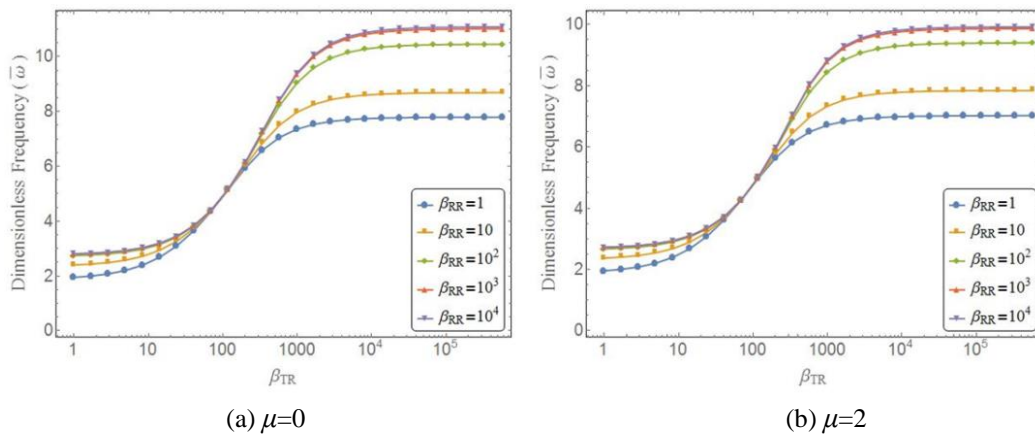


Fig. 8 The variation of the first dimensionless frequency of P-FG nanobeam with spring constant factors for different non-locality parameters with C-E boundary conditions ($L/h=20, p=0.5$)

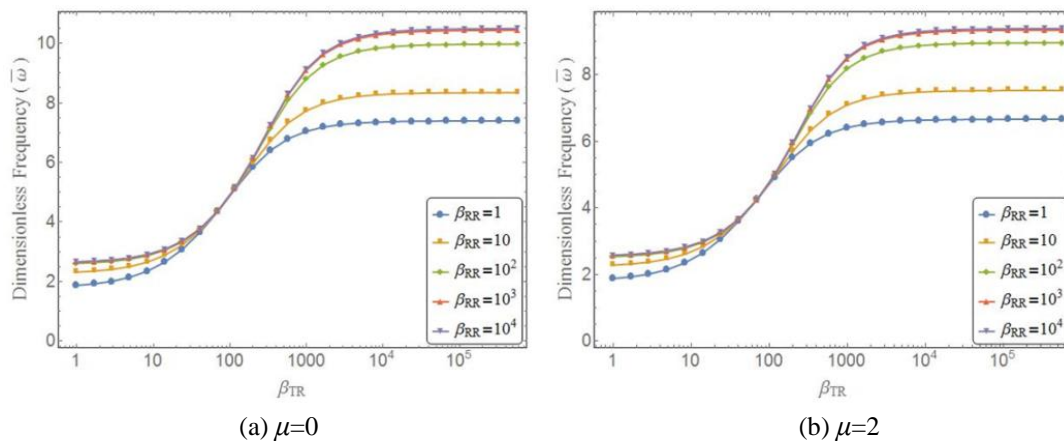


Fig. 9 The variation of the first dimensionless frequency of S-FG nanobeam with spring constant factors for different non-locality parameters with C-E boundary conditions ($L/h=20, p=0.5$)

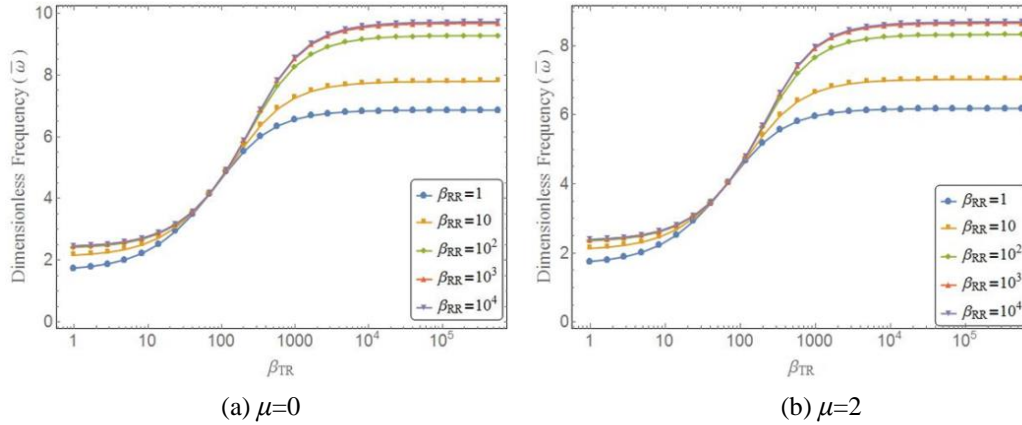


Fig. 10 The variation of the first dimensionless frequency of MT-FG nanobeam with spring constant factors for different non-locality parameters with C-E boundary conditions ($L/h=20, p=0.5$)

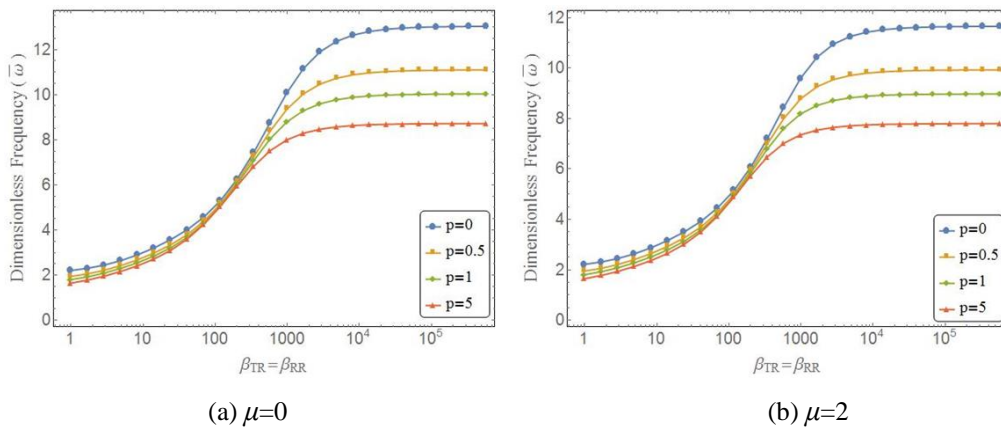


Fig. 11 The variation of the first dimensionless frequency of P-FG nanobeam with spring constant factor and material graduation for different non-locality parameters with C-E boundary conditions ($L/h=20$)

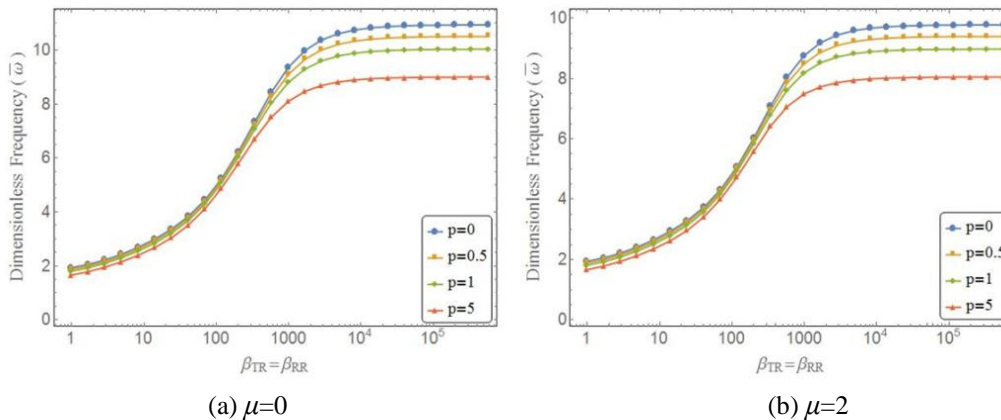


Fig. 12 The variation of the first dimensionless frequency of S-FG nanobeam with spring constant factor and material graduation for different non-locality parameters with C-E boundary conditions ($L/h=20$)

It is revealed that for fixed values of β_{RR} the considerable increase of the frequencies is found in the range of moderate spring stiffness from 10 to 10^3 . Also, it is deduced that the fundamental frequency increases by increasing β_{RR} and it can be stated that spring constant factors has a significant effect on the fundamental frequency of the graded nanobeam.

The other important parameter in vibration behavior of nonlocal FG beam is its gradient index parameter. Figs. 11 and 12 are dedicated to study the variation of dimensionless fundamental frequencies of FG beams with spring constant factors and nonlocal parameters by using both the material compositions (P-FGM and S-FGM), which are clamped at left end and supported by elastic springs at another end.

Inspection of these figures reveals that an increase in the value of the power exponent leads to a decrease in the fundamental frequencies. Comparing the frequency values for FG nanobeams with various non-classical boundary conditions presented in Tables 10 and 11 reveals that for a prescribed nonlocal parameter and gradient index the greatest frequency, is obtained for the FG beam with C-E boundary conditions followed with S-E nanobeams. Furthermore, the effects of

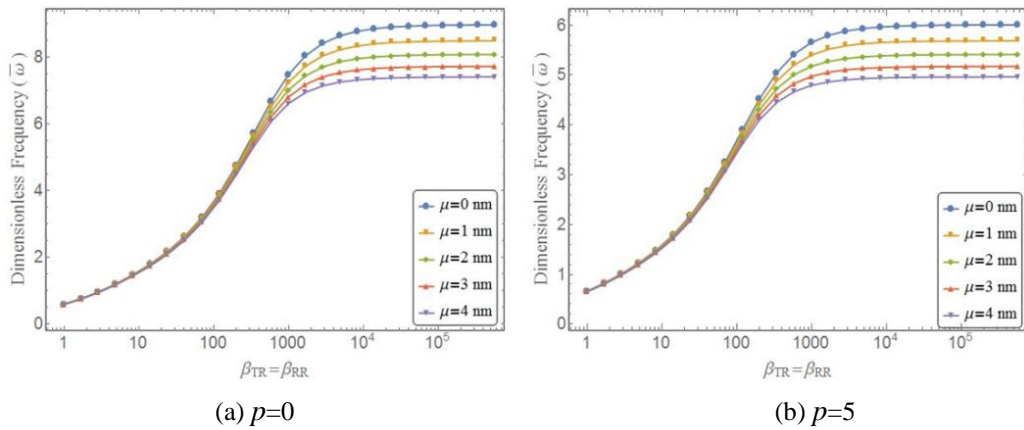


Fig. 13 The variation of the first dimensionless frequency of P-FG nanobeam with spring constant factor and nonlocality parameters for different gradient indexes with S-E boundary conditions ($L/h=20$)

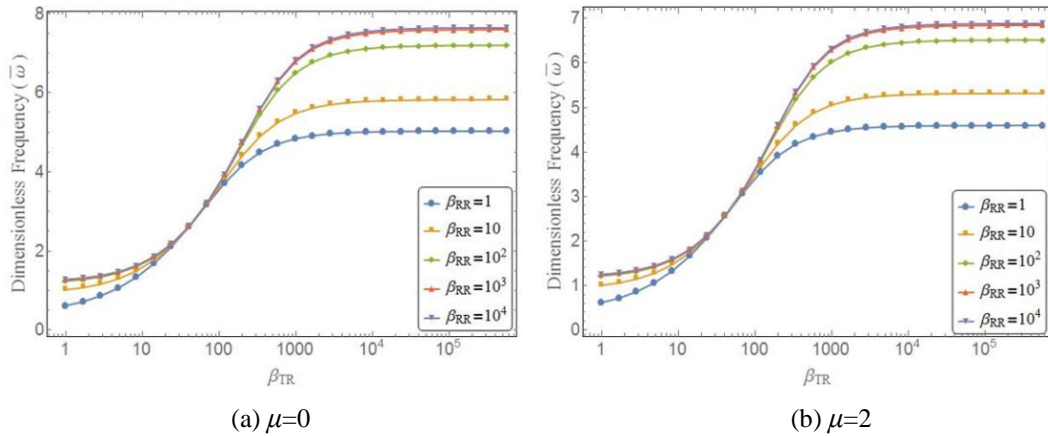


Fig. 14 The variation of the first dimensionless frequency of P-FG nanobeam with spring constant factors for different non-locality parameters with S-E boundary conditions ($L/h=20, p=0.5$)

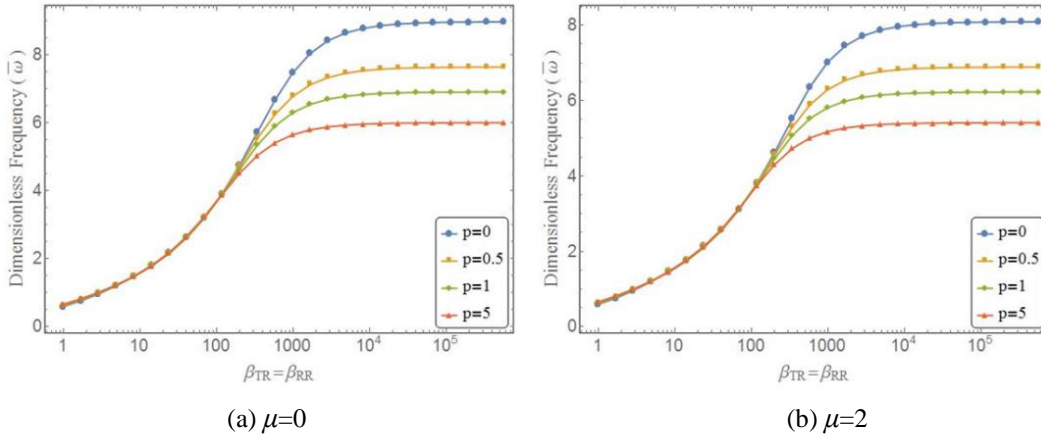


Fig. 15 The variation of the first dimensionless frequency of P-FG nanobeam with spring constant factor and material gradation for different non-locality parameters with S-E boundary conditions ($L/h=20$)

spring constant factors, nonlocal parameter and gradient indexes on the dimensionless frequencies are presented in these tables.

The last analysis deals with the material gradation and nonlocal parameter effect on vibration behavior of S-E FG nanobeam with different spring constant factors.

The variation of the first dimensionless frequency of P-FG nanobeam with spring constant factors and non-locality parameters for different material gradation are plotted in Figs. 13-15. Similar to two previously discussed edge conditions, it is revealed that for a S-E FG nanobeam increasing power index, and nonlocal parameter, leads to decrease in natural frequency. Besides, for higher values of spring constant factors, graded nanobeam becomes stiffer and thus, the dimensionless fundamental frequency increases while the spring constant increases.

6. Conclusions

In this paper, vibrational behavior of the FG nanobeams supported by various classical and non-classical boundary conditions is investigated on the basis of nonlocal elasticity theory in conjunction with differential transform method. Eringen’s theory of nonlocal elasticity together with Euler–Bernoulli beam theory is used to model the nanobeam. The material’s properties of the FG nanobeams are assumed to vary continuously through the thickness according to P-FGM, S-FGM and MT-FGM models. The governing differential equations and related boundary conditions are derived by implementing Hamilton’s principle. Implementing the differential transformation technique, the governing partial differential equation is reduced to algebraic equations. Accuracy of the results is examined using available data in the literature, for some cases of the FG beams with classical and non-classical boundary conditions. Finally, through some parametric study and numerical examples, the effect of different parameters is investigated. The effects of small scale parameter, material property gradient index and spring constant factors on fundamental frequencies of FG nanobeams with elastic supports including translational and rotational springs are investigated. It is concluded that various factors such as nonlocal parameter, gradient index and spring constant factors play important roles in dynamic behavior of FG

nanobeams with both classical and non-classical boundary conditions. It is illustrated that presence of non-locality leads to reduction in natural frequency. It is observed that the fundamental frequency increases with the increase in rotational and translational springs. However, in the range of soft springs, it can be concluded there are slight difference in value of the frequency results of nonlocal FGM beam, for every material compositions. Also, it is concluded, with the increase in the gradient index value leads to the decrease in frequency. Moreover it is revealed that, in terms of classical boundary condition, the greatest frequency is obtained for the FG nanobeam with C–C boundary conditions followed with C-S, S-S and C-F, respectively.

References

- Alshorbagy, A.E., Eltahir, M.A. and Mahmoud, F.F. (2011), “Free vibration characteristics of a functionally graded beam by finite element method”, *Appl. Math. Model.*, **35**(1), 412-425.
- Ansari, R., Gholami, R. and Sahmani, S. (2011), “Free vibration analysis of size-dependent functionally graded microbeams based on the strain gradient Timoshenko beam theory”, *Compos. Struct.*, **94**(1), 221-228.
- Asghari, M., Ahmadian, M.T., Kahrobaiyan, M.H. and Rahaeifard, M. (2010), “On the size-dependent behavior of functionally graded micro-beams”, *Mater. Des.*, **31**(5), 2324-2329.
- Asghari, M., Rahaeifard, M., Kahrobaiyan, M.H. and Ahmadian, M.T. (2011), “The modified couple stress functionally graded Timoshenko beam formulation”, *Mater. Des.*, **32**(3) 1435-1443.
- Aydogdu, M. (2009), “A general nonlocal beam theory: its application to nanobeam bending, buckling and vibration”, *Physica E: Low-dimen. Syst. Nanostr.*, **41**(9), 1651-1655.
- Belabed, Z., Houari, M.S.A., Tounsi, A., Mahmoud, S. and Bég, O.A. (2014), “An efficient and simple higher order shear and normal deformation theory for functionally graded material (FGM) plates”, *Compos. Part B: Eng.*, **60**, 274-283.
- Bennoun, M., Houari, M.S.A. and Tounsi, A. (2016), “A novel five-variable refined plate theory for vibration analysis of functionally graded sandwich plates”, *Mech. Adv. Mater. Struct.*, **23**(4), 423-431.
- Besseghier, A., Heireche, H., Bousahla, A.A., Tounsi, A. and Benzair, A. (2015), “Nonlinear vibration properties of a zigzag single-walled carbon nanotube embedded in a polymer matrix”, *Adv. Nano Res.*, **3**(1), 029.
- Bounouara, F., Benrahou, K.H., Belkorissat, I. and Tounsi, A. (2016), “A nonlocal zeroth-order shear deformation theory for free vibration of functionally graded nanoscale plates resting on elastic foundation”, *Steel Compos. Struct.*, **20**(2), 227-249.
- Chemi, A., Heireche, H., Zidour, M., Rakrak, K. and Bousahla, A.A. (2015), “Critical buckling load of chiral double-walled carbon nanotube using non-local theory elasticity”, *Adv. Nano Res.*, **3**(4), 193-206.
- Civalek, Ö., Cigdem, D., and Bekir, A. (2010), “Free vibration and bending analyses of cantilever microtubules based on nonlocal continuum model”, *Math. Comput. Appl.*, **15**(2), 289-298.
- Eltahir, M.A., Alshorbagy, A.E. and Mahmoud, F.F. (2013), “Determination of neutral axis position and its effect on natural frequencies of functionally graded macro/nanobeams”, *Compos. Struct.*, **99**, 193-201.
- Eltahir, M.A., Emam, S.A. and Mahmoud, F.F. (2012), “Free vibration analysis of functionally graded size-dependent nanobeams”, *Appl. Math. Comput.*, **218**(14), 7406-7420.
- Eltahir, M.A., Emam, S.A. and Mahmoud, F.F. (2013), “Static and stability analysis of nonlocal functionally graded nanobeams”, *Compos. Struct.*, **96**, 82-88.
- Eringen, A.C. (1972), “Nonlocal polar elastic continua”, *Int. J. Eng. Sci.*, **10**(1), 1-16.
- Eringen, A.C. (1983), “On differential equations of nonlocal elasticity and solutions of screw dislocation and surface waves”, *J. Appl. Phys.*, **54**(9) 4703-4710.
- Hamidi, A., Houari, M.S.A., Mahmoud, S. and Tounsi, A. (2015), “A sinusoidal plate theory with 5-unknowns and stretching effect for thermomechanical bending of functionally graded sandwich plates”,

- Steel Compos. Struct.*, **18**(1), 235-253.
- Hebali, H., Tounsi, A., Houari, M.S.A., Bessaim, A. and Bedia, E.A.A. (2014), "New quasi-3D hyperbolic shear deformation theory for the static and free vibration analysis of functionally graded plates", *J. Eng. Mech.*, **140**(2), 374-383.
- Hosseini-Hashemi, S. and Nazemnezhad, R. (2013), "An analytical study on the nonlinear freevibration of functionally graded nanobeams incorporating surface effects", *Compos. Part B: Eng.*, **52**, 199-206.
- Ke, L.L. and Wang, Y.S. (2011), "Size effect on dynamic stability of functionally gradedmicrobeams based on a modified couple stress theory", *Compos. Struct.*, **93**(2), 342-350.
- Ke, L.L., Wang, Y.S., Yang, J. and Kitipornchai, S. (2012), "Nonlinear free vibration ofsize-dependent functionally graded microbeams", *Int. J. Eng. Sci.*, **50**(1), 256-267.
- Ma'en, S.S. and Butcher, E.A. (2012), "Free vibration analysis of non-rotating and rotatingTimoshenko beams with damaged boundaries using the Chebyshev collocation method", *Int. J. Mech. Sci.*, **60**(1), 1-11.
- Mahmoud, S., Chaht, F.L., Kaci, A., Houari, M.S.A., Tounsi, A. and Bég, O.A. (2015), "Bending and buckling analyses of functionally graded material (FGM) size-dependent nanoscale beams including the thickness stretching effect", *Steel Compos. Struct.*, **18**(2), 425.
- Pradhan, S.C. and Murmu, T. (2010), "Application of nonlocal elasticity and DQM in the flap wise bending vibration of a rotating nano cantilever", *Physica E: Low-dimen. Syst. Nanostr.*, **42**(7), 1944-1949.
- Shahba, A., Attarnejad, R., Marvi, M.T. and Hajilar, S. (2011), "Free vibration and stability analysisof axially functionally graded tapered Timoshenko beams with classical and non-classical boundary conditions", *Compos. Part B: Eng.*, **42**(4), 801-808.
- Sharabiani, P.A. and Yazdi, M.R.H. (2013). (2013), "Nonlinear free vibrations of functionally graded nanobeams with surface effects", *Compos. Part B: Eng.*, **45**(1), 581-586.
- Şimşek, M. (2010), "Fundamental frequency analysis of functionally graded beams by using different higher-order beam theories", *Nucl. Eng. Des.*, **240**(4), 697-705.
- Tounsi, A., Benguediab, S., Adda, B., Semmah, A. and Zidour, M. (2013), "Nonlocal effects on thermal buckling properties of double-walled carbon nanotubes", *Adv. Nano Res.*, **1**(1), 1-11.
- Tounsi, A., Bourada, M., Kaci, A. and Houari, M.S.A. (2015), "A new simple shear and normal deformations theory for functionally graded beams", *Steel Compos. Struct.*, **18**(2), 409.
- Wang, Q. (2005), "Wave propagation in carbon nanotubes via nonlocal continuum mechanics", *J. Appl. Phys.*, **98**(12), 124301.
- Wang, Q., and Varadan, V.K. (2006), "Vibration of carbon nanotubes studied using nonlocal continuum mechanics", *Smart Mater. Struct.*, **15**(2), 659.
- Wattanasakulpong, N. and Variddhi, U. (2014), "Linear and nonlinear vibration analysis ofelastically restrained ends FGM beams with porosities", *Aerosp. Sci. Tech.*, **32**(1), 111-120.
- Witvrouw, A. and Mehta, A. (2005), "The use of functionally graded poly-SiGe layers for MEMS applications", *Materials science forum*, **492**, Trans Tech Publications.
- Zemri, A., Houari, M.S.A., Bousahla, A.A. and Tounsi, A. (2015), "A mechanical response of functionally graded nanoscale beam: an assessment of a refined nonlocal shear deformation theory beam theory", *Struct. Eng. Mech.*, **54**(4), 693-710.
- Zhang, Y.Q., Liu, G.R. and Wang, J.S. (2004), "Small-scale effects on buckling of multiwalled carbon nanotubes under axial compression", *Phys.Rev. B*, **70**(20), 205430.